Scripta Materialia 194 (2021) 113660

Contents lists available at ScienceDirect

Scripta Materialia

journal homepage: www.elsevier.com/locate/scriptamat

Anomalous compliance of interpenetrating-phase composite of Ti and Mg synthesized by liquid metal dealloying

Ilya Vladimirovich Okulov[a,b,c,d,*], Jana Wilmers[e], Soo-Hyun Joo[f], Swantje Bargmann[e,g], Hyoung Seop Kim[h], Hidemi Kato[a]

[a] Institute for Materials Research, Tohoku University, Katahira 2-1-1, Sendai 980-8577, Japan
[b] Institute of Natural Sciences, Ural Federal University, 620000 Ekaterinburg, Russia
[c] Faculty of Production Engineering, University of Bremen, Badgasteiner Str. 1, 28359 Bremen, Germany
[d] Leibniz Institute for Materials Engineering - IWT, Badgasteiner Str. 3, 28359 Bremen, Germany
[e] Chair of Solid Mechanics, University of Wuppertal, Gaußstr. 20, 42119 Wuppertal, Germany
[f] Department of Materials Science and Engineering, Dankook University, 119 Dandae-ro, Cheonan 31116, Korea
[g] Wuppertal Center for Smart Materials & Systems, University of Wuppertal, 42119 Wuppertal, Germany
[h] Department of Materials Science and Engineering Pohang University of Science and Technology 77 Cheongam-Ro, 37673 Pohang, South Korea

ARTICLE INFO

Article history:
Received 11 November 2020
Accepted 4 December 2020
Available online 14 December 2020

Keywords:
Low modulus
Effective Properties
Composite
Porous
Dealloying

ABSTRACT

Low modulus biomaterials are in focus as potential candidates for biomedical implants ensuring a fast healing of hard tissues. The close match between elastic properties of an implant material and bone are critical to eliminate stress-shielding effect. In this study, we synthesized a low modulus interpenetrating-phase composite of Ti and Mg by liquid metal dealloying. Its Young's modulus value is in the range of that found for human bone which allows for biomedical applications of this material. Unexpectedly, the Young's modulus value of the composite (17.6 GPa) is several times lower than that of each individual constituent phases, namely, Mg (45 GPa) and Ti (110 GPa). Using micromechanical modelling, it is demonstrated that the origin of the anomalously low modulus can be related to a weakened interface between the constituents.

Dealloying-based interpenetrating-phase composites demonstrate significant deviation of their mechanical behaviour from that estimated using various rules of mixtures [1–3]. The interpenetrating-phase composites of nanoporous metal and polymer, for example, are substantially stronger and harder than the nanoporous metal or polymer individually [2–6]. Moreover, these metal-polymer composites exhibit extremely low modulus compared with expectations while still falling between the Voigt-Reuss bounds [3,4]. In a recent study, it was demonstrated that the Young's modulus of the dealloying-based composite consisting of Fe and Mg is significantly lower than each constituent. This anomalous behaviour is associated with interfacial phenomena [1]. This particular phenomenon (anomalous reduction of the Young's modulus) was also observed for other in-situ and ex-situ composites obtained by different methods including as-cast in-situ composite of Mg metallic glass and steel [7], composite of Mg and TiNi obtained by infiltration [8], ex-situ composite of Mg metallic glass and Ti_2B synthesized by casting [9], and others. The origin of the anomalously low Young's modulus in the dealloying-based interpenetrating-phase composites remains unexplored to a high extent.

In nanoscale materials, interfaces and interfacial areas can have a significant effect on the material's effective mechanical properties, resulting in a strong size effect [10,11]. Analysis of this size effect predicts a softening of the material if the interfaces are weakened or imperfectly bonded. Modelling using interface elasticity theory finds a significant reduction of Young's modulus compared to perfect cohesion for inclusion composites with large interface-to-volume ratios [12,13]. The magnitude of the effect depends on the structure morphology and the characteristic length scale – with increasing structure size, interfacial influence on the effective modulus vanishes. The characteristic length scale in the recent dealloying-based Fe-Mg composite possessing anomalously low effective elastic modulus [1] is in the micron scale regime and is several orders of magnitude higher compared to the above mentioned nanomaterials [14] which might indicate a different origin of low modulus.

* Corresponding author.
E-mail address: okulovilya@yandex.ru (I.V. Okulov).

https://doi.org/10.1016/j.scriptamat.2020.113660

To gain insights into the nature of the low elastic modulus in the dealloying-based interpenetrating-phase composites, the composite of Ti and Mg was synthesized by liquid metal dealloying [15–17]. Liquid metal dealloying is the metallurgical method implying selective dissolution of one (or more) element(s) form the precursor alloys immerced in liquid metal and formation of an interpenetrating-phase microstructured composite [16,18]. This method is mainly used for synthesis of open porous materials [19,20,36–40] and surface functionalisation [21,22]. However, directly after liquid metal dealloying, an interpenetrating-phase composite is formed and porous materials are synthesized in a subsequent step by chemical etching of the composite [6,23]. In this study, the microstructure and mechanical behavior of the current dealloying-based Ti-Mg composite were characterised in detail. The obtained information was used for the micromechanical computational model which provided new insights into the phenomenon of low modulus in dealloying-based interpenetrating-phase composites.

The interpenetrating-phase composite of Ti and Mg was synthesized by liquid metal dealloying from the precursor $Ti_{50}Cu_{50}$ (at%) alloy. The precursor alloy was prepared from pure metals, namely, Ti and Cu (99.99 %), using arc-melting device under Ar atmosphere. Thereafter, the precursor alloy was cast into the rectangular ($6 \times 30 \times 70$ mm^3) copper crucible. The as-cast precursor alloy samples was cut into 1 mm thick slices for liquid metal dealloying. To obtain the composite of Ti and Mg, the precursor alloy was dealloyed in liquid magnesium at 1073 K for 20 min. The open porous titanium samples were synthesized by chemical etching of the composite in 3 M HNO_3 for 5 h. During the chemical etching, the Mg phase dissolves from the composite of Ti and Mg. Structural investigation of the composite and porous samples was performed by X-ray diffraction in Bragg-Brentano geometry (SmartLab, Regaku, Japan) with Cu-K$_\alpha$ radiation. The microstructure and chemical composition were explored using scanning electron microscopy (SEM, Gemini Ultra 55, Karl Zeiss, Germany) coupled with energy-dispersive X-ray analysis (Bruker, Germany). For the mechanical tests, the rectangular $1 \times 1 \times 2$ mm^3 compression test samples were fabricated by diamond saw. The mechanical behaviour of the composite and porous samples was probed at room temperature and at the strain rate of 10^{-4} s^{-1} using a universal testing machine (Z010 TN, Zwick-Roell, Germany). The strain was computed from the relative displacement of the load surfaces as measured by a laser extensometer (LaserXtens, Zwick). The yield strength was determined at the 0.002 offset strain.

The effective Young's modulus of interpenetrating phase composites is assessed by micromechanical modelling of a unit cell. The composite is modelled as interpenetrating orthogonal branching structures with rectangular cross-sections. Using a step-wise homogenisation scheme, the unit cell's effective properties are calculated. Each unit cell is subdivided into 3×3 subcells consisting of three material blocks. These subcells are aligned along the assumed loading direction and homogenised under the uniform stress assumption. In a second step, the nine subcells are homogenised under the assumption of uniform strain. The Young's moduli are $E_{TI} = 110\,\text{GPa}$ and $E_{Mg} = 45\,\text{GPa}$ and the Poisson's ratios of both phases are assumed to be 0.3. The effective properties of a porous phase are modelled using a differential homogenisation scheme for homogenously distributed spherical pores [24]. The differential homogenisation is solved numerically and the effective Young's modulus of the unit cell is determined using an in-house code implemented in Python.

The dealloying-based Ti-Mg composite mainly consists of hexagonal close-packed (hcp) α-Ti and hcp Mg phases (Fig. 1). There is also some minor amount of an intermetallic Mg_2Cu phase found in the composite. Fig. 2 depicts the microstructure and elemental mapping of the Ti-Mg composite. The SEM and EDX analyses reveal three different phases, namely, micron scale Ti and Mg phases as well as submicron scale Mg-rich phase containing Cu (Fig. 2c). Due to the fine microstructure of the Mg-rich phase, the accurate determination of its composition was impossible using EDX analysis. According to the XRD and SEM analysis as well as the Mg(Cu) phase diagram [25], it can be assumed that the residual Cu diffused into the Mg melt during dealloying process promoted the formation of the eutectic structure. The eutectic structure consists of the Mg_2Cu and Mg phases what have been reported previously in [26].

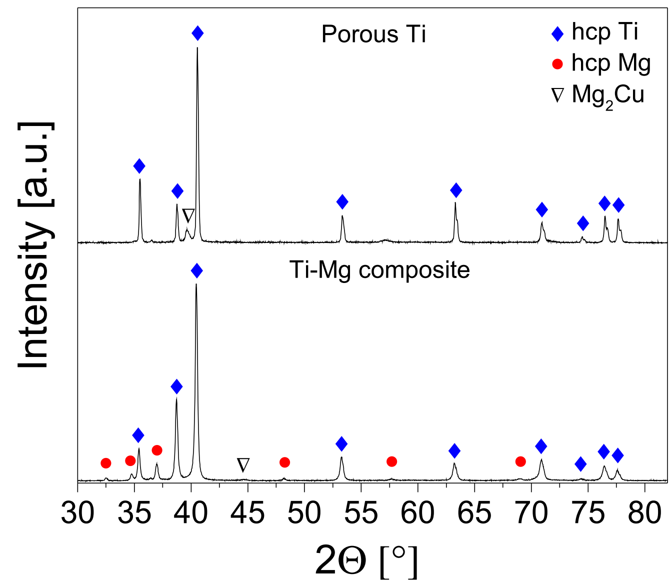

Fig. 1. XRD diffractograms of the porous Ti and Ti-Mg composite samples

Porous Ti was obtained by etching of the Mg phase from the Ti-Mg composite. According to XRD analysis shown in Fig. 1, porous Ti consists of hcp α-Ti and a minor amount of the Mg_2Cu phase. The Mg_2Cu phase seems to be resistant to 3M HNO_3 aqueous solution.

Fig. 3 presents mechanical properties of the porous Ti and the Ti-Mg composite samples probed under compression loading. For each material the two stress-strain curves demonstrate very good reproducibility. The porous Ti exhibits an excellent plastic deformability and, therefore, the compression test of this material was aborted at the strain of about 0.7. The yield strength of the porous Ti reaches about 35 ± 3 MPa. The Young's modulus of the porous Ti is about 3.3 ± 0.3 GPa. Due to presence of the Mg phase, the Ti-Mg composite is less ductile compared to the porous Ti sample. It fractures at a compression strain of about 0.23 ± 0.03. However, the strength characteristics of the Ti-Mg composite are significantly improved. The yield and maximum strength values of the Ti-Mg composite reach about 180 ± 10 MPa and 410 ± 40 MPa. The manifold increase of strength of the Ti-Mg composite as compared to the porous Ti is due to change of the deformation mode [2]. As reported in [27], the deformation of the dealloying-based porous metals is mainly governed by bending and torsion of individual ligaments. Introduction of a second phase prevents bending deformation and leads to the stretching-contraction dominant deformation and, thus, higher strength performance [28].

As the distinguished feature of the Ti-Mg composite its Young's modulus is unexpectedly low. The Young's modulus value is about 17.6 ± 0.5 GPa (Table 1) what is below that of the individual constituent materials, namely, titanium and magnesium. The Young's modulus values of hcp α-Ti and hcp Mg is about 110 GPa [29] and 45 GPa [30], respectively. The anomalously low Young's modulus values were reported for the interpenetrating-phase TiNi-Mg com-

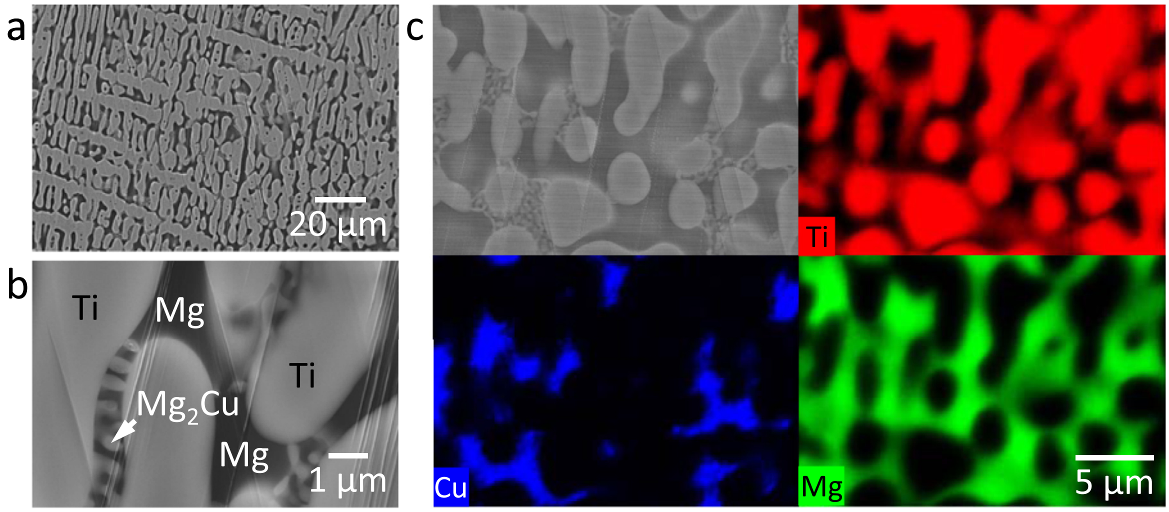

Fig. 2. Secondary electron micrographs (a and b) and elemental mapping (c) of the Ti-Mg composite.

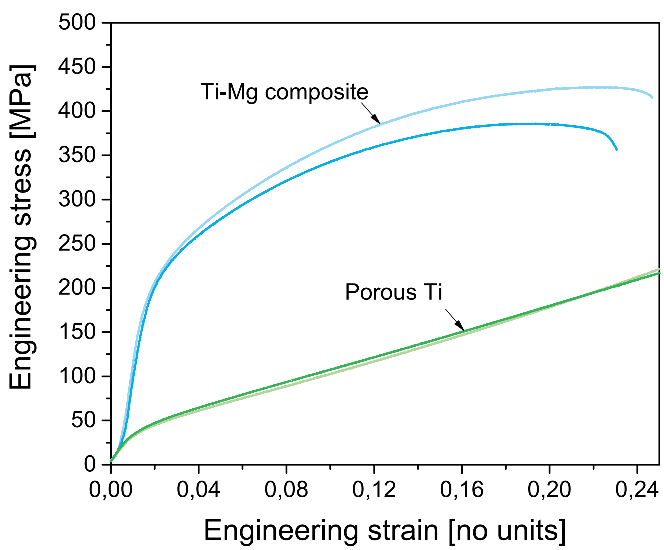

Fig. 3. Mechanical behavior of the porous Ti and the Ti-Mg composite samples.

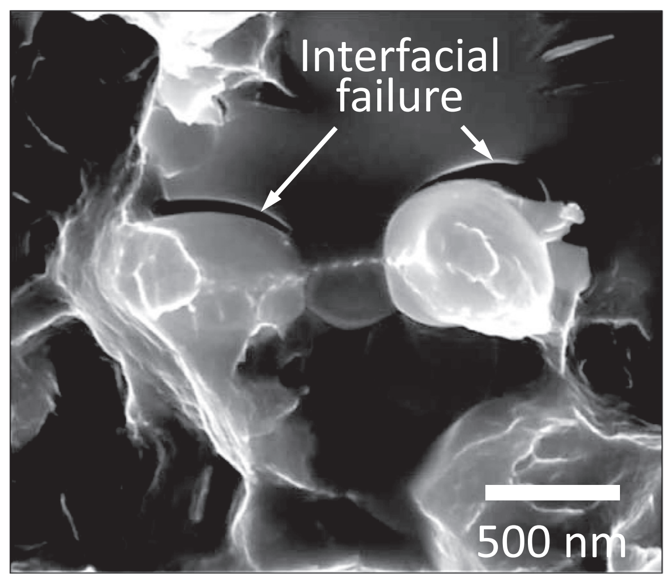

Fig. 4. Secondary electron micrograph of the fracture surface of the Ti-Mg composite after compression test. The deadhesion of Ti and Mg phases along the interfaces is clearly visible.

Table 1
Mechanical properties of the porous Ti and Ti-Mg composite samples probed under compression.

Sample	Yield strength (MPa)	Young's modulus (GPa)
Porous Ti	35 ± 3	3.3 ± 0.3
Ti-Mg composite	180 ± 10	17.6 ± 0.5

posite (25 GPa) fabricated by infiltration of liquid Mg into the open porous TiNi scaffold [31] and for the dealloying-based Fe-Mg composite (20 GPa) [1]. In both cases, the composites were probed under compression loading. The low modulus was associated with the weak interface between constituent phases for the Fe-Mg composite due to dissimilar nature of these metals. Their weak interface leads to grain boundary sliding upon compression loading and, therefore, a low Young's modulus value [1]. Similar to the Fe-Mg composite, the interface between Ti and Mg phases of the Ti-Mg composite seems to be weak as a result of their dissimilar nature [25]. Additionally, the coefficient of volumetric thermal expansion of Mg (78 10^{-6} K^{-1}) is 3 times higher than that of Ti (26 10^{-6} K^{-1}) [29,30] and Mg shrinks by 4.2 vol% upon liquid to solid transformation. Although porosity in the Ti-Mg composite was undetected by SEM analysis, the unequal shrinkage of materials upon cooling might lead to formation of a nanoscale porosity and internal stresses supporting interfacial weakening. The evidence of the interfacial boundaries weakness is shown in Fig. 4 showing the fracture surface of a Ti-Mg compressive sample. The deadhesion of the Ti and Mg phases along the interfaces is clearly visible.

The dominant effect interfaces may have on mechanical properties of nanoscale materials is well-documented and theoretically described using the principles of interface elasticity theory for perfect interfaces as well as interface sliding [5,14,32,33]. However, the volume-specific interface area of the Ti-Mg composite as estimated from stereological assessment of micrographs is with $\alpha \approx 0.7 \mu m^{-1}$ multiple orders of magnitude lower than in nanoporous metals [34] or nanocrystalline metals [14]. Pure interface elasticity theory, thus, suggests only a minor interface influence on the composite's behaviour. Residual interface stresses could increase this effect and the occurrence of porosity localised close to the interface may similarly promote a softening of the composite.

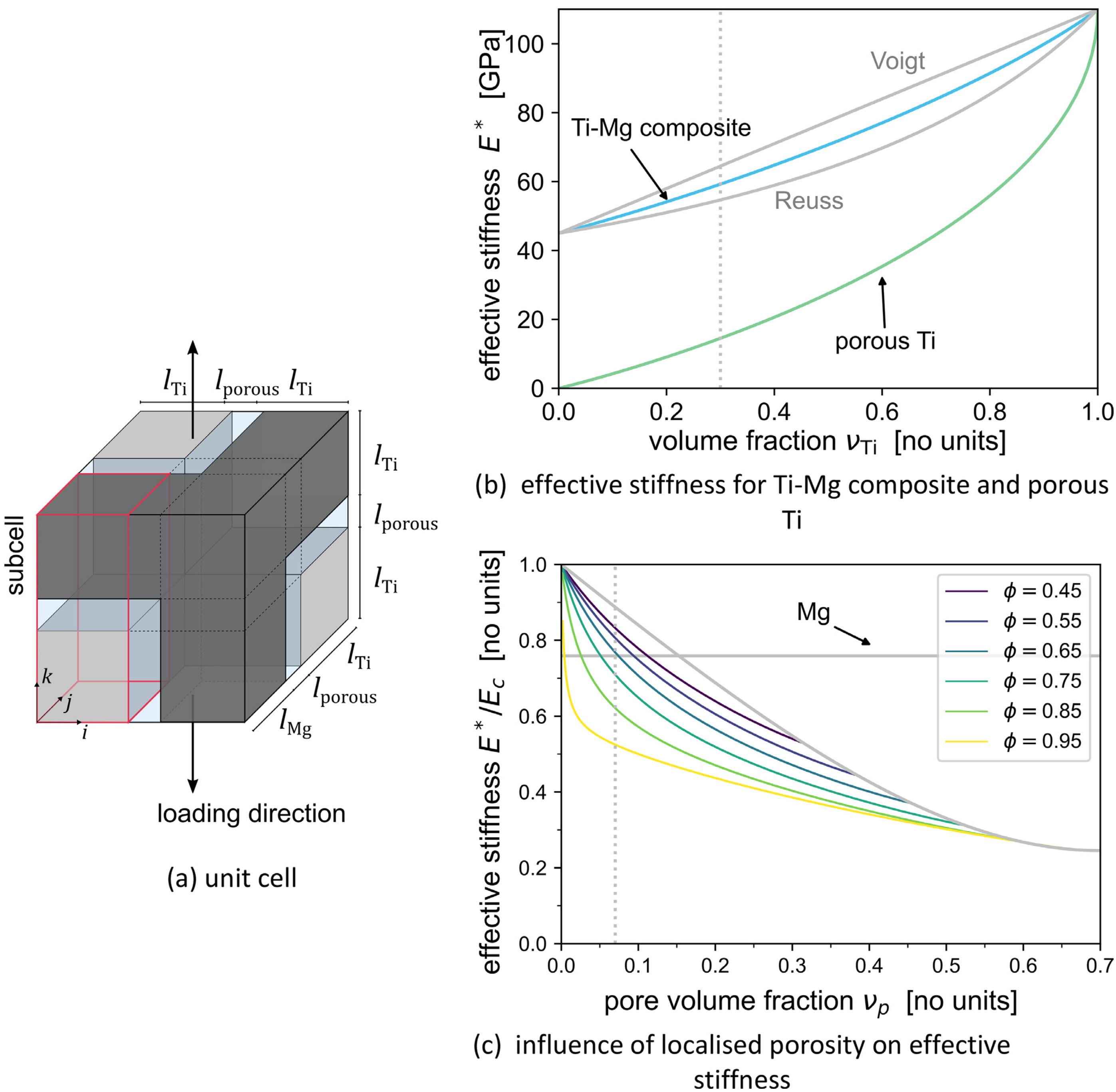

Fig. 5. An idealised unit cell of an interpenetrating composite of Ti and Mg (a) is used to model the composite's effective properties. A layer of porous Mg (blue) is located at the interface between both. (b) Effective stiffness for Ti-Mg composite without any pores or interface imperfections and porous Ti and (c) Ti-Mg composite (30 vol% of Ti) exhibiting a local porosity Φ in the porous layer.

To investigate the effect even a moderate amount of porosity can have on the interpenetrating-phase composites' stiffness if it is localised close to the interface, a unit cell as depicted in Fig. 5 a is considered. This volume element represents a co-continuous composite consisting of three separate regions: Ti, Mg and a layer of porous Mg. As suggested in [35], the effective Young's modulus E^* of the unit cell can be calculated analytically from a decomposition into $3 \times 3 \times 3$ differently sized blocks (dotted lines in Fig. 5) each belonging to only one material region. Three blocks aligned in loading direction form a subcell (indicated in red in Fig. 5). Each subcell is homogenised under the uniform stress assumption. The subcells are then combined assuming uniform strain within the whole cell. The effective Young's modulus E^* of the composite is calculated from

$$E^* = \sum_{i=1}^{3}\sum_{j=1}^{3}\left[\left[\left[\sum_{k=1}^{3}\frac{V_{ijk}}{E_{ijk}}\right]^{-1}\sum_{k=1}^{3}V_{ijk}\right]\sum_{k=1}^{3}\frac{V_{ijk}}{V_{cell}}\right], \tag{1}$$

as the porous layer thickness l_{porous} are the same on every edge, resulting in isotropic composite behaviour.

With Eq. (1), the effective Young's modulus of the composite with zero porosity is determined to be$E^*_c = 59.3\,\text{GPa}$ at a volume fraction of Ti of $\nu_{Ti} = 30\%$. Fig. 5b depicts the variation of the estimated stiffness of the Ti-Mg composite with different proportions of phases and without any porosity. The model's predictions fall between the Voigt-Reuss bounds (grey lines in Fig. 5b), i.e., the predictions of the theory of mixtures. For comparison, the predicted stiffness of porous Ti is also given. At $\nu_{\mathrm{Ti}} = 30\%$, a stiffness of $E^*_{porous\mathrm{Ti}} = 14.5\,\mathrm{GPa}$ is obtained which is much stiffer than the experimentally found value $E^*_{porous\mathrm{Ti}} = 3.3\,\mathrm{GPa}$. This is expected, as the model cannot account for the bending dominated deformation of porous structures. Yet, the chosen model structure takes into account the interconnectivity of the individual phases as well as their interpenetrating morphology. In the following, the absolute values are not considered and instead all predictions are normalised by the effective stiffness of the perfect binary composite E^*_c.

If unequal shrinkage during cooling results in the formation of small pores in the composite, these pores will be localised close to the interface. The influence of a local porosity ϕ up to 95 % in a thin layer of Mg at the interface is investigated here. To estimate the properties of the porous Mg, a differential homogenisation scheme assuming an even distribution of spherical pores in the layer [24] is applied. The differential homogenisation scheme takes into account the interaction ofϕ neighbouring pores.

Porosity results in local softening between the two solid metal phases. Increasing the local porosity , thus, results in an increase of the total volume fraction of pores ν_p in the element and a reduction of the effective stiffness. Figure 5 c depicts the results for a composite with a Ti volume fraction of $\nu_{\mathrm{Ti}} = 30\%$. The grey line in Fig. 5 c denotes the case of a solid Ti phase fully filled with porous Mg. With increasing porosity, the effective modulus drops at a moderate rate towards the properties of porous Ti, falling below the stiffness of either of the metal constituents at a global porosity of ca. 15 %. For 7 % total porosity, the stiffness is only ca. 89 % of the perfect composite's stiffness E^*_c. The same amount of global porosity localised in a thin layer between non-porous Ti and Mg phases can however result in an even more drastic reduction of stiffness. For a total porosity of 7 % localized in a layer with 95 % porosity, the composite's stiffness drops to approximately half of the binary composite's despite two perfect, interconnected metal phases being present.

It is evident from Fig. 5 c that even moderate porosity has a drastic influence on the material's overall behaviour if it is localised and, thus, weakens the interface considerably. Due to the simplified example structure, the model predictions cannot be analysed quantitatively, but they evidentiary highlight the significant influence localised porosity and weakened interfaces have on a composite's stiffness, resulting in the anomalously low modulus of the interpenetrating-phase composite of Ti and Mg.

In summary, the interpenetrating-phase composite of Ti and Mg has been synthesized from the precursor $Ti_{50}Cu_{50}$ (at%) alloy by liquid metal dealloying. The unique feature of the Ti-Mg composite is anomalously low Young's modulus of 17.6 ± 0.5 GPa (several times lower than that of each constituent) combined with a moderate yield strength of 180 ± 10 MPa. The origin of the anomalously low modulus in the Ti-Mg composite is associated with the weak interface between constituent Ti and Mg phases. This hypothesis was proved by means of micromechanical modelling. The result of the modelling suggests that even moderate porosity in the interpenetrating-phase Ti-Mg composite imposes a drastic effect on the composite's overall behavior if it is localised, e.g., homogeneously distributed, along the interface. This localised porosity is likely due to shrinkage of the Mg phase upon solidification as well as unequal shrinkage of the Ti and Mg phases upon cooling due to unequal coefficients of volumetric thermal expansion.

Declaration of Competing interest

The authors declare that they have no known competing financial interests or personal relationships that could have appeared to influence the work reported in this paper.

Acknowledgement

The authors are grateful to Prof. Mädler for valuable discussions. The financial support was provided by the International Collaboration Center, Institute for Materials Research (ICC-IMR), Tohoku University, Japan and the German Science Foundation under the Leibniz Program (Grant MA 3333/13-1).

Reference

[1] I.V. Okulov, P.-A. Geslin, I.V. Soldatov, H. Ovri, S.-H. Joo, H. Kato, Scr. Mater 163 (2019) 133–136.
[2] K. Wang, J. Weissmüller, Adv. Mater 25 (2013) 1280–1284.
[3] I.V. Okulov, J. Weissmüller, J. Markmann, Sci. Rep 7 (2017) 20.
[4] A.V. Okulov, A.S. Volegov, J. Weissmüller, J. Markmann, I.V. Okulov, Scr. Mater 146 (2018) 290–294.
[5] J. Wilmers, S. Bargmann, Extrem. Mech. Lett 21 (2018) 57–64.
[6] I.V. Okulov, A.V. Okulov, A.S. Volegov, J. Markmann, Scr. Mater 154 (2018) 68–72.
[7] H. Ma, J. Xu, E. Ma, Appl. Phys. Lett 83 (2003) 2793–2795.
[8] W. Guo, H. Kato, Mater. Des 83 (2015) 238–248.
[9] Y.-K. Xu, H. Ma, J. Xu, E. Ma, Acta Mater 53 (2005) 1857–1866.
[10] P. Sharma, S. Ganti, J. Appl. Mech 71 (2004) 663–671.
[11] H.L. Duan, J. Wang, Z.P. Huang, B.L. Karihaloo, J. Mech. Phys. Solids 53 (2005) 1574–1596.
[12] H. Le Quang, Q.-C. He, Mech. Mater 40 (2008) 865–884.
[13] S. Firooz, G. Chatzigeorgiou, F. Meraghni, A. Javili, Mech. Mater 139 (2019) 103204.
[14] J. Weissmüller, J. Markmann, M. Grewer, R. Birringer, Acta Mater 59 (2011) 4366–4377.
[15] T. Wada, K. Yubuta, A. Inoue, H. Kato, Mater. Lett 65 (2011) 1076–1078.
[16] P. Geslin, I. Mccue, J. Erlebacher, A. Karma, Nat. Commun 6 (2015) 1–19.
[17] S.-H. Joo, J.W. Bae, W.-Y. Park, Y. Shimada, T. Wada, H.S. Kim, A. Takeuchi, T.J. Konno, H. Kato, I.V. Okulov, Adv. Mater 32 (2020) 1906160.
[18] T. Wada, T. Ichitsubo, K. Yubuta, H. Segawa, H. Yoshida, H. Kato, Nano Lett 14 (2014) 4505–4510.
[19] A.V. Okulov, S.-H. Joo, H.S. Kim, H. Kato, I.V. Okulov, Metals 10 (2020) 1396 Basel.
[20] I.V. Okulov, A.V. Okulov, I.V. Soldatov, B. Luthringer, R. Willumeit-Römer, T. Wada, H. Kato, J. Weissmüller, J. Markmann, Mater. Sci. Eng. C 83 (2018) 95–103.
[21] Y. Fukuzumi, T. Wada, H. Kato, in: K. Sasaki, O. Suzuki, N. Takahashi (Eds.), Springer Japan, Tokyo, 2015, pp. 93–101.
[22] I.V. Okulov, S.-H. Joo, A.V. Okulov, A.S. Volegov, B. Luthringer, R. Willumeit-Römer, L. Zhang, L. Mädler, J. Eckert, H. Kato, Nanomaterials 10 (2020).
[23] I.V. Okulov, S.V Lamaka, T. Wada, K. Yubuta, M.L. Zheludkevich, J. Weissmüller, J. Markmann, H. Kato, Nano Res 11 (2018) 6428–6435.
[24] S. Giordano, Eur. J. Mech. - A/Solids 22 (2003) 885–902.
[25] H. Baker (Ed.), ASM Handbook: Alloy Phase Diagrams, ASM International, Materials Park, 1992.
[26] M. Tsuda, T. Wada, H. Kato, J. Appl. Phys 114 (2013) 113503.
[27] B. Roschning, N. Huber, J. Mech, Phys. Solids 92 (2016) 55–71.
[28] E. Griffiths, S. Bargmann, B.D. Reddy, Extrem. Mech. Lett 17 (2017) 16–23.
[29] C. Leyens, M. Peters, Titanium and Titanium Alloys, WILEY-VCH Verlag GmbH & Co. KGaA, Weinheim, 2003.
[30] K.U. Kainer, F. Buch, Magnesium - Alloys and Technology, WILEY-VCH Verlag GmbH & Co. KGaA eds, Weinheim, 2004.
[31] W. Guo, H. Kato, Mater. Lett 158 (2015) 1–4.
[32] M.E. Gurtin, A. Ian Murdoch, Arch. Ration. Mech. Anal 57 (1975) 291–323.
[33] J. Wilmers, A. McBride, S. Bargmann, J. Mech, Phys. Solids 99 (2017) 163–177.
[34] N. Mameka, Surface-Controlled Mechanical Properties of Bulk Nanoporous Gold, Technische Universität Hamburg (2016).
[35] X.-Q. Feng, Z. Tian, Y.-H. Liu, S.-W. Yu, Appl. Compos. Mater 11 (2004) 33–55.
[36] M. Mokhtari, T. Wada, C. Le Bourlot, N. Mary, J. Duchet-Rumeau, H. Kato, E. Maire, Low cost high specific surface architectured nanoporous metal with corrosion resistance produced by liquid metal dealloying from commercial nickel superalloy, Scr. Mater. 163 (2019) 5–8, doi:10.1016/j.scriptamat.2018.12.023.
[37] S.A. Berger, I.V. Okulov, Open porous $\alpha + \beta$ titanium alloy by liquid metal dealloying for biomedical applications, Metals (Basel) 10 (2020) 1450, doi:10.3390/met10111450.
[38] S.-H. Joo, K. Yubuta, H. Kato, Ordering kinetics of nanoporous FeCo during liquid metal dealloying and the development of nanofacets, Scr. Mater. 177 (2020) 38–43, doi:10.1016/j.scriptamat.2019.10.007.
[39] T. Wada, P. Geslin, H. Kato, Preparation of hierarchical porous metals by two-step liquid metal dealloying, Scr. Mater. 142 (2018) 101–105, doi:10.1016/j.scriptamat.2017.08.038.
[40] T. Wada, H. Kato, Three-dimensional open-cell macroporous iron, chromium and ferritic stainless steel, Scr. Mater. 68 (2013) 723–726, doi:10.1016/j.scriptamat.2013.01.011.